FOSSEE, IIT Bombay
OpenFOAM Case Study Project
June 2024

Flow Around a Cylinder: A Comparative Study of Immersed Boundary and Arbitrary Lagrangian–Eulerian (ALE) Methods in OpenFOAM

Antim Gupta[1] and Chandan Bose[2]

[1]Faculty of Technology, Design and Environment, Oxford Brookes University, Wheatley, Oxford, OX33 1HX, United Kingdom
[2]Assistant Professor, Aerospace Engineering, College of Engineering and Physical Sciences, The University of Birmingham

June 4, 2024

Synopsis

This study presents a comparative analysis of flow around a cylinder using the Immersed Boundary Method (IBM) and the Arbitrary Lagrangian-Eulerian (ALE) approach within the OpenFOAM® (FOAM-Extend-4.1) computational fluid dynamics framework. IBM simplifies mesh generation by utilizing a fixed Cartesian grid, whereas ALE accommodates dynamic mesh deformation. We performed 2D transient numerical simulations for Reynolds numbers (Re = 100, 200, 1000, 2000) to evaluate the accuracy, efficiency, and robustness of both methods in capturing key flow characteristics such as vortex shedding, lift, and drag coefficients. Both static and oscillating cylinder flows were investigated. Initially, mesh sensitivity analysis was conducted using Richardson extrapolation with a refinement factor of 2 and was validated against existing literature [1] [2] [3] [4] [5] for Re = 200. The results demonstrate that both methods can accurately simulate flow around a cylinder, though they differ in computational efficiency and ease of implementation. IBM required significantly more computational time to achieve result convergence compared to ALE. For static cylinders, ALE studies included IcoFoam-laminar, PimpleFoam-laminar, and PimpleFoam with the k-omega SST turbulence model. The laminar models were effective for low Reynolds numbers (≤200), producing a drag coefficient (Cd) of 1.4 for Re = 100 and 200 using IcoFoam, and 1.38 and 1.375 using PimpleFoam-laminar. The k-omega SST model estimated Cd values of 1.37 and 1.29 for Re = 1000 and 2000, respectively. Using IBM with the IcoFoam solver, Cd values were 1.5, 1.44, 1.287, and 1.143 for Re = 100, 200, 1000, and 2000, respectively. Studies on oscillating cylinder flows, considering a 0.1D amplitude in the y-axis at a frequency of 1Hz, are also presented and compared for IBM and ALE at Re = 100, alongside time-dependent and grid sensitivity tests for

IBM. These findings provide insights into the strengths and limitations of IBM and ALE methods, emphasizing trade-offs between computational efficiency and implementation complexity. Future work will explore three-dimensional flows and hybrid approaches to combine the advantages of both methods.

1 Introduction

Understanding the flow physics around cylindrical objects is a fundamental problem in fluid dynamics with numerous engineering applications, including aerospace, civil, and mechanical engineering sector [6]. Cylindrical structures are commonly used in various engineering designs such as bridge piers, pipelines, offshore platforms for turbines and oil drilling, and aerodynamic bodies like aircraft components and turbine blades [7]. Accurate simulation of such flows is crucial for designing efficient structures and devices subjected to fluid forces, as it directly impacts their aerodynamic performance, safety, and durability [8]. Predicting vortex-induced vibrations and drag forces on cylindrical structures can lead to better designs that mitigate structural fatigue and failure caused by resonance frequency [9], [10].

The flow around a cylindrical object changes significantly with different Reynolds numbers (Re), a dimensionless parameter indicating the relative significance of inertial forces to viscous forces in a fluid flow [11]. The formation of different von Kármán vortex streets with respect to Reynolds number for the flow around circular cylinder is illustrated below:

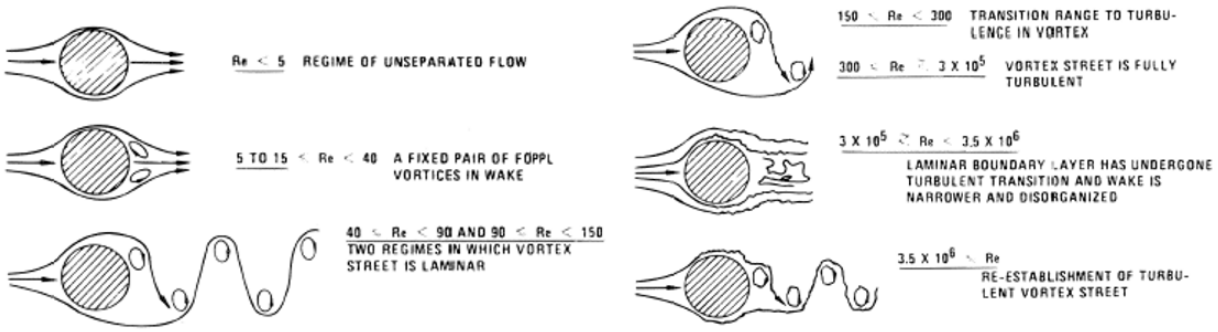

Figure 1: Formation of Von Kármán vortex streets around cylinder at different Reynolds number [12].

The aerodynamic performance of any object depends on the Reynolds Number (Re) [13]; As Re increases:

- At Re < 5, the flow remains attached and symmetrical with no separation.
- Between Re 5 to 15, steady, symmetric Eppil vortices form behind the cylinder.
- For Re 40 to 150, periodic vortex shedding occurs, creating a laminar von Kármán vortex street.
- In the range of Re 150 to 300, the flow transitions from laminar to turbulent, increasing instability.

- At Re 300 to 3 $\times 10^5$, the vortex street becomes fully turbulent with chaotic shedding.
- Between Re 3 $\times 10^5$ to 3.5 $\times 10^6$, the wake becomes narrower and more disorganized as the laminar boundary layer transitions to turbulence.
- For Re > 3.5 $\times 10^6$, a fully turbulent vortex street is re-established.

There are various ways to study the aerodynamic performance and flow characteristics of the flow around circular cylinder at different Reynolds numbers, including wind tunnel tests, field tests, high-fidelity modeling using computational fluid dynamics (CFD), and low-fidelity modeling using analytical equations. Computational fluid dynamics (CFD) models provide high-resolution data similar to experimental tests without the need to create prototypes, making them more cost-effective compared to expensive and time-consuming wind tunnel and field tests. The flow filed are computed computationally using CFD [14].

Two prominent computational methods for simulating flow around cylinders are the Immersed Boundary Method (IBM) and the Arbitrary Lagrangian-Eulerian (ALE) approach. IBM simplifies the mesh generation process by allowing complex geometries to be represented on a fixed or base Cartesian grid, thus avoiding the need for dynamic mesh adaptation. This method is particularly useful for simulations involving moving boundaries or deformable structures. However, the simplicity of IBM comes at the cost of increased computational time to achieve convergence, especially for high-fidelity simulations [15].

The Immersed Boundary Method was first implemented in Foam-Extend 3.2 and Foam-Extend 4.0 based on the Discrete Ghost-Cell Forcing approach with a weighted least squares interpolation. However, Foam-Extend version 4.1 is based on the discrete cut cell approach and offers greater accuracy in capturing flow characteristics. In Foam-Extend 4.1, cells within IBM are categorized into three types after intersection: fluid (live), solid (dead), and intersected cells, as shown in Figure 2. Unlike previous versions, Foam-Extend 4.1 considers all intersected cells as IB cells, not just those whose centers are in the fluid region, as illustrated below [16], [17]:

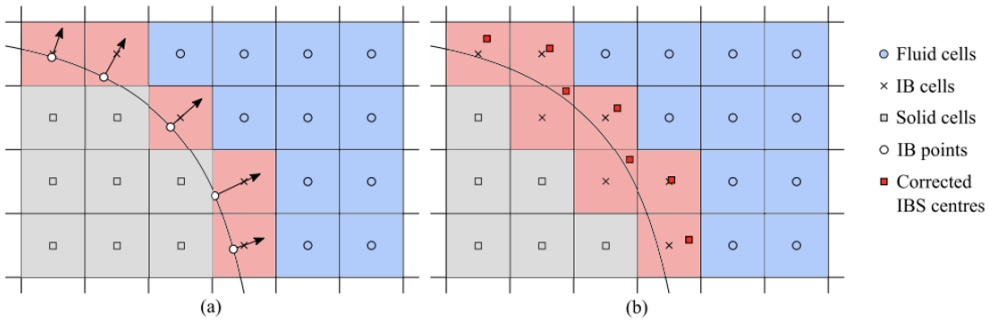

Figure 2: Cell types for IBM in a) Foam-Extend 4.0 and b) Foam-Extend 4.1 [17]

The Immersed Boundary (IB) method utilizes linear cuts through intersection points within each cell. Cells are divided into living (fluid) and dead (solid) sections. The living sections become independent fluid cells, rather than being added to neighboring cells as in traditional cut-cell methods. This approach necessitates new calculations for cell center, volume, and geometrical data

for cut faces and new IB faces. Dead cells and faces are excluded from the discretization matrix. Geometric data for the living parts of the cells are updated, enabling the IB influence to be incorporated as a standard boundary condition in finite volume method discretization [16], as shown below:

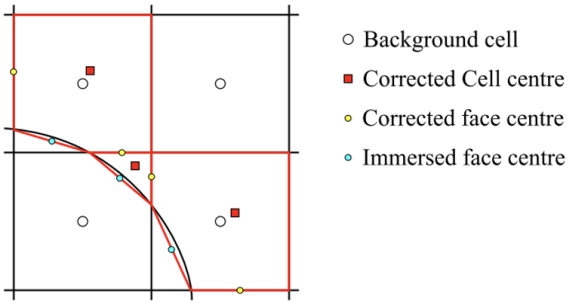

Figure 3: Cut-Cells with corrected cells and face centers by Foam-Extend 4.1 [16]

Foam-Extend 4.1 has great potential to solve both simple static mesh and dynamic mesh problems, including transient or steady-state simulations. The static mesh solvers include laplacianFoam, simpleFoam, and icoFoam. For dynamic mesh problems, the PIMPLE method, referred to as pimpleDyMIbFoam, is used. Regardless of the solver employed, the manipulation of the discretization matrix is primarily handled in two IB classes [15], [16]:

- immersedBoundaryPolyPatch
- immersedBoundaryFvPatch

For the immersed boundaries, the cutting and manipulation of geometrical information are performed at the level of polyPatch data by the immersedBoundaryPolyPatch class. Meanwhile, the immersedBoundaryFvPatch class serves as the connection between the immersed boundary condition and the finite volume discretization.

The Arbitrary Lagrangian-Eulerian (ALE) CFD technique is good at handling mesh changes during simulations, which helps in accurately capturing boundary layer effects and flow separation [18]. ALE is useful when precise control over the mesh near object boundaries is needed, such as in studies of laminar-turbulent transition and complex wake dynamics. This method provides accurate results for flow characteristics like vortex shedding and drag coefficients and is widely used in both academic and industrial applications [19]. However, implementing ALE can be complex and computationally demanding, requiring advanced mesh generation and handling techniques. The ALE approach involves cutting cells to define fluid and solid boundaries, making it possible to simulate fluid-solid interactions within the CFD framework. It solves moving domain problems within a fixed reference domain by using an artificial domain velocity. This approach applies the characteristic method to solve the Navier-Stokes equations in the fixed domain, ensuring accurate simulation results [20], [21].

This report presents a comparative study of the Immersed Boundary Method (IBM) and the Arbitrary Lagrangian-Eulerian (ALE) methods within the OpenFOAM computational fluid dynamics framework. The study investigates the flow around static cylinders at various Reynolds numbers

(Re = 100, 200, 1000, 2000) to evaluate the accuracy, efficiency, and robustness of both methods. Initial mesh sensitivity analyses, employing Richardson extrapolation, were performed and validated against existing literature [1] [2] [3] [4] [5] for Re = 200. Additionally, this study analyzes the flow around oscillating cylinders with a 0.1D amplitude in the y-axis at a frequency of 1.5 Hz to understand the dynamic response and the effect of grid independence using IBM. The oscillation of the cylinder was set up using the dynamic mesh capabilities of OpenFOAM, and the IBM studies were conducted using the OpenFOAM Foam-Extend version 4.1.

By comparing the two methods, this study aims to highlight the strengths and limitations of each approach, providing insights into their applicability for various fluid dynamics problems. The findings will inform future research and practical applications, guiding the selection of appropriate computational methods for specific engineering challenges.

2 Governing Equations and Models

2.1 Problem definition

The objective of this study is to model and analyze the flow around a cylinder, emphasizing wake characteristics and aerodynamic performance using CFD. It compares the ALE approach (OpenFOAM version 9) with the IBM (Foam-Extend version 4.1). Both static and oscillating cylinders are examined to assess differences in wake dynamics, boundary layer behavior, and aerodynamic coefficients between the two methods.

2.2 Governing equations

In this study, both laminar and turbulent models have been analyzed for the flow around a cylinder. In CFD, the flow fields are computed using the conservation equations of mass and momentum for incompressible and isothermal fluid flow, coupled with the energy equation. The mathematical expressions for the conservation of mass and momentum, also referred to as the incompressible Navier-Stokes (N-S) equations [22], are given by:

$$\frac{\partial u}{\partial x} + \frac{\partial v}{\partial y} + \frac{\partial w}{\partial z} = 0 \tag{1}$$

$$\rho \left[\frac{\partial u_i}{\partial t} + u_j \frac{\partial u_i}{\partial x_j} \right] = -\frac{\partial P}{\partial x_i} + \mu \frac{\partial^2 u_i}{\partial x_j x_j} + \rho g_i \tag{2}$$

The N-S equations above are solved simultaneously using a finite volume-based solver with fluid flow boundary conditions. To accurately capture the effects of turbulence on fluid flow with higher Reynolds numbers, a Reynolds Averaged Navier-Stokes (RANS) model is utilized. RANS models decompose instantaneous velocity into mean and fluctuating components, and the time-averaged solution is used to reduce the equations [22], as demonstrated below:

$$\frac{\partial \rho u_i}{\partial t} + \frac{\partial \rho u_i u_j}{\partial x_j} = -\frac{\partial P}{\partial x_i} + \mu \frac{\partial^2 u_i}{\partial x_j \partial x_j} - \frac{\partial \overline{\rho u_i' u_j'}}{\partial x_j} + \rho g_i \tag{3}$$

The Reynolds stress term $-\overline{\rho u_i' u_j'}$, represented by a turbulence eddy viscosity (μ_t) model, follows the shear-stress-transport (SST) $k-\omega$ model. This model has accurate boundary layer capturing capabilities at transitional flow .

2.3 Geometry and Mesh

A rectangular domain was chosen as the control volume (CV) with dimensions of 50 meters in the x-direction and 40 meters in the y-direction. The cylinder is located at origin (0, 0, 0), has a diameter of 2 meters and is positioned 20 meters away from the left boundary of the domain. The top and bottom walls were kept far from the cylinder to minimize boundary effects on its aerodynamic performance [23], as illustrated below:

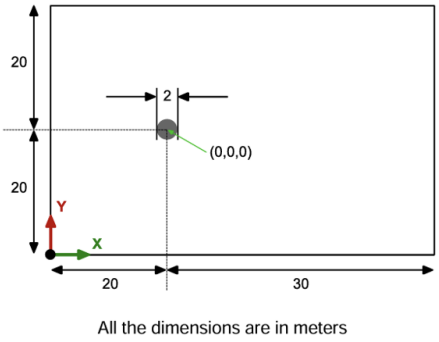

Figure 4: Control Volume domain choosen for this study

The control volume dimensions for both ALE and IBM studies were kept the same. The geometry was modelled in OpenFOAM using a blockMeshDict file and a structured mesh was generated for both solvers. Edge grading was used to refine the mesh near the cylinder, and smooth grading was applied to ensure a gradual transition between blocks, avoiding sudden jumps in cell size and ensuring smooth fluid flow field calculations. The block mesh for both the ALE and IBM solver are illustrated below:

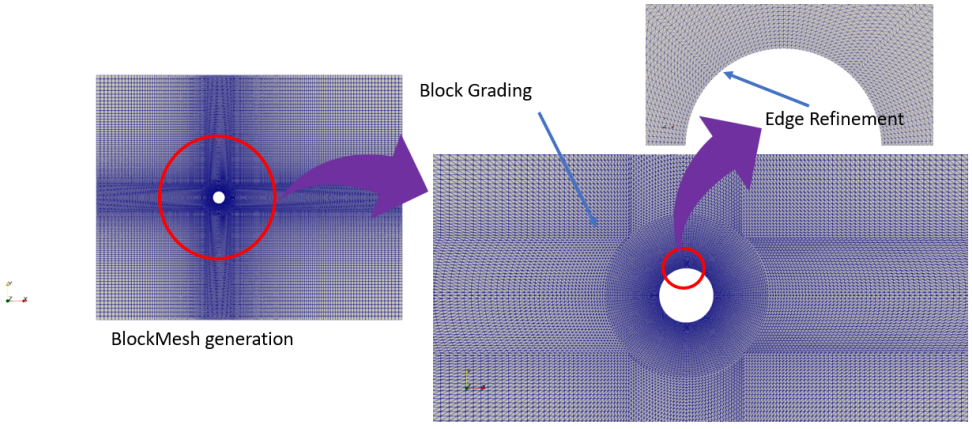

Figure 5: BlockMesh used for ALE approach.

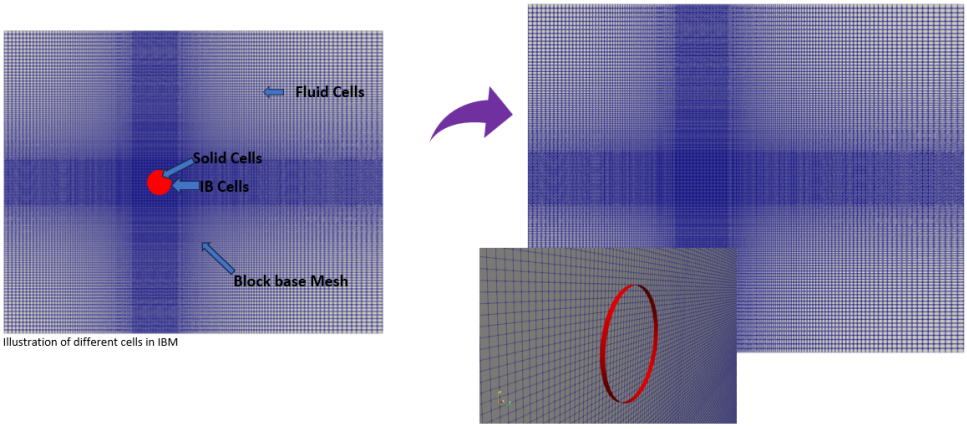

Figure 6: BlockMesh used for IBM approach.

In ALE modeling, the cylindrical patch was cut to define the boundary of the object for fluid-structure interaction (FSI). However, for IBM, a base structured mesh was generated, and an IB cylinder surface was created separately using On-Shape (online CAD modeling site) to define the immersed boundary solid walls inside the domain without actually cutting the cells. The domain cells are then categorized into solid cells, IB cells, and fluid cells within the base mesh.

2.4 Initial and Boundary Condition

For the ALE approach, the initial and boundary conditions for the CFD simulation included fixed velocity and zero gradient pressure at the inlet in the x-direction, inletOutlet velocity and fixed pressure at the outlet to maintain zero atmospheric output pressure, symmetry conditions on the top and bottom walls, no-slip wall conditions at the cylinder walls, and empty face type for front and back faces due to 2D simulation. The initial and boundary condition for ALE approach are illustrated below:

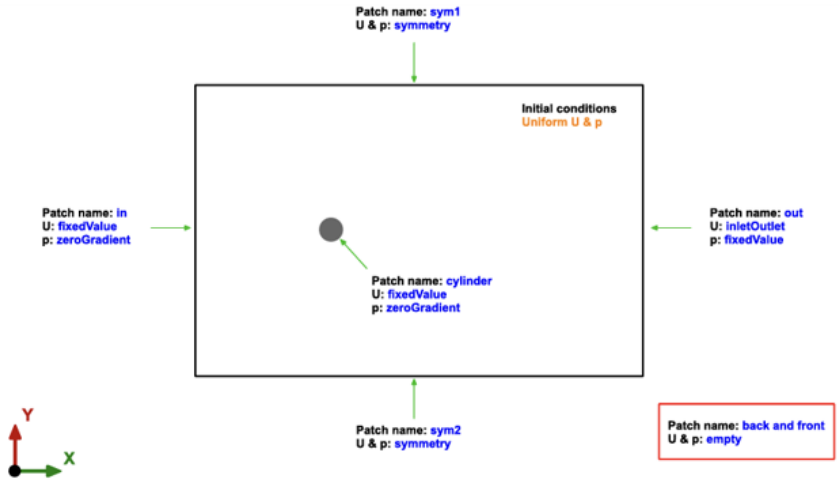

Figure 7: Initial and Boundary conditions for ALE model

However for the Immersed Boundary Method (IBM) approach, the cylinder surface as defined as an immersed solid boundaries (ibCylinder) using a mixedIb type biundary condition. The front and back planes are set to empty for both studies. Uniform initial conditions for velocity and pressure are applied throughout the domain. The initial and boundary condition for IBM approach are illustrated below:

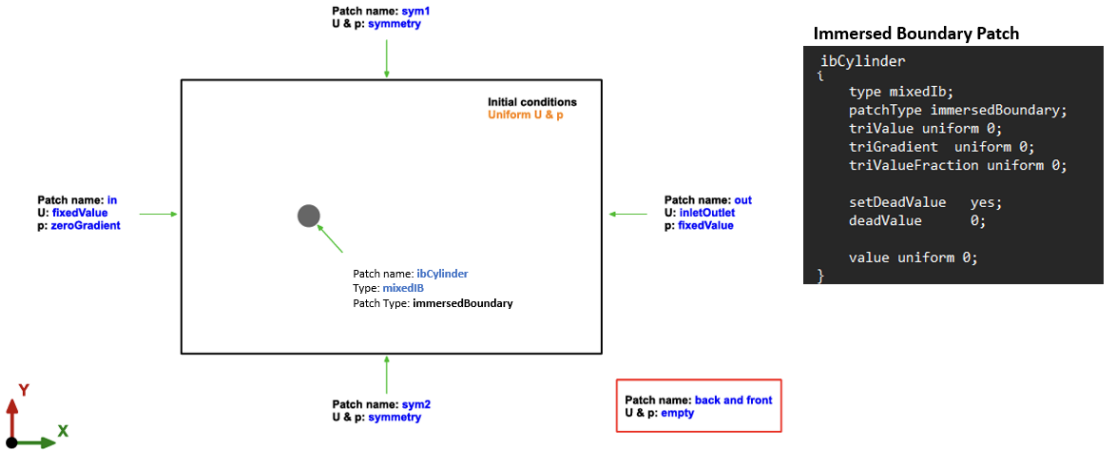

Figure 8: Initial and Boundary conditions for IBM model

2.5 Solver setup

2.5.0.1 Fluid Properties

A in-compressible Newtonian fluid is used to study the effect of varying Reynolds numbers for the flow around a cylinder. The density is set to 1 kg/m^3, and the kinematic viscosity is varied to achieve different Reynolds numbers: 0.02 m^2/s for Re=100, 0.01 m^2/s for Re=200, 0.002 m^2/s for Re=1000, and 0.001 m^2/s for Re=2000. This adjustment of viscosity allows for the control of the Reynolds number, ensuring the correct flow characteristics. The Newtonian transport model is utilized in the transport properties of the fluid to maintain consistent behavior in accordance with the Newtonian fluid assumption.

2.5.0.2 Dynamic Mesh Treatment

In this study, the oscillating cylinder CFD model parameters were carefully chosen to analyze the dynamic behavior of the cylinder under varying conditions. The oscillating amplitude was set to 0.1D, where D represents the diameter of the cylinder (m) for oscilatting frequency of 1 Hz. The simulations were conducted for Re=100, using two solvers: PimpleFoam for the Arbitrary Lagrangian-Eulerian approach and pimpleDyMFoam for the Immersed Boundary Method This approach ensured that the dynamic mesh treatment accurately captured the fluid-structure interactions and provided reliable data for comparison between the ALE and IBM methods. The setup and parameters are summarized in Table 1 below:

Table 1: Oscillating Cylinder CFD Model Parameters

Parameter		
Oscillating Amplitude	0.1D	D = Diameter of Cylinder (m)
Oscillating Frequency	F= 1 Hz	
Solver	PimpleFoam (ALE)	pimpleDyMFoam (IBM)
Re	100	

For the ALE model, the dynamic mesh treatment was configured using the PimpleFoam solver in OpenFOAM version 9. displacementLaplacian solver with quadratic diffusivity type was used in dynamic mesh dictionary (dynamicMeshDict) to ensure smooth mesh adaptation around the oscillating cylinder. A additional pointDisplacement file is used to define the cylinder's oscillating motion/physics, with the oscillatingDisplacement type applied to the cylinder boundary for forced displacement. Dynamic mesh motion is specified for the boundaries with the required amplitude and oscillation frequency. This setup allows the mesh to dynamically adapt to the cylinder's motion, accurately capturing fluid-structure interactions.

For the IBM model, the pimpleDyMFoam in Foam-Extend version 4.1 is used with defined oscillating parameters. The dynamic mesh parameters are configured using the dynamicMeshDict file. The dynamic mesh type is set as immersedBoundarySolidBodyMotionFvMesh, which enables dynamic motion for the immersed boundary. The motion function for the cylinder, named ibCylinder, is defined using the linearOscillation function type. The oscillation parameters are set with an amplitude of (0, 0.1D, 0), indicating a 0.1D (meter) unit oscillation in the Y-direction for a specific period. This configuration enables the cylinder to undergo linear oscillation with the specified amplitude and period. This setup is essential for accurately capturing fluid-structure interactions and simulating the oscillatory behavior of the cylinder within the fluid domain considering Immersed Boundary Methods.

2.5.0.3 Solution Method and Control

For IBM: The simulation control parameters were configured using the controlDict file. In this study, we explored two solvers, namely pimpleDyMFoam and icoFoam, by incorporating the immersedBoundary libraries. A small time step was selected for all simulations to precisely capture the detailed transient flow characteristics and vortex structures. Transient solvers were utilized to study the time-variation behavior of flow physics around the cylinder. Forces on the cylinder were measured using the inbuilt force function, facilitated by the libforces.so library. Solution methods were defined in the fvSolution file to specify the solvers and algorithms necessary for solving the governing equations. The pressure-velocity coupling was managed using the 'SIMPLE' algorithm, with adjustments for non-orthogonality and under-relaxation to enhance convergence. Solvers for pressure and velocity fields were respectively configured with CG (Conjugate Gradient) and BiCGStab (Bi-Conjugate Gradient Stabilized) methods, supplemented by appropriate preconditioners to ensure numerical stability and efficiency. Numerical discretization strategies were set using the fvSchemes file. Time derivatives were approximated using the Euler method, while spatial discretizations employed Gauss linear schemes for gradient calculations and upwind schemes for divergence terms, ensuring both accuracy and stability in capturing the complex dynamics of the flow. These schemes were crucial for accurately resolving the interactions between the fluid and

the cylinder, enabled by IBM.

For ALE: Three solvers, namely Laminar-pimpleFoam, laminarIcoFoam, and pimpleFoam-kOmegaSST turbulence model, were used in this study to capture the transient flow physics around the cylinder. Forces were reported using the inbuilt force function. Numerical discretization was set up in the fvSchemes files to maintain the accuracy and stability of the computations. The 'Euler' scheme was chosen for time derivatives, and gradient calculations were performed using the least squares method. Divergence and Laplacian schemes were carefully selected to balance computational efficiency and numerical precision, which are critical for managing the complex flow dynamics around the cylinder. The finite volume solution was handled by the fvSolution file. Different solvers were utilized for pressure and velocity fields, with GAMG employed to enhance efficiency during the coarse levels of the simulation and PCG used for the final pressure adjustments. Velocity was managed by a PBiCGStab solver with specific preconditioners to ensure solver robustness. The PIMPLE algorithm was configured to optimize the coupling between pressure and velocity fields, accommodating the dynamic mesh adjustments intrinsic to the ALE method used in the simulation.

3 Results and Discussions

3.1 Convergence Tests

3.1.1 Grid Size Convergence Test

A mesh or grid size convergence test is important for evaluating the impact of mesh refinement on the accuracy and stability of computational fluid dynamics (CFD) simulations. In this study, the Richardson extrapolation technique was utilized to conduct the mesh sensitivity analysis, wherein the element size was refined by a factor of 2, thereby minimizing errors associated with mesh refinment. The flow around a static cylinder at a Reynolds number (Re) of 200 was analsysed by employing both Arbitrary Lagrangian-Eulerian (ALE) and Immersed Boundary Method (IBM) approaches. Four different mesh quality were generated using the blockMeshDict file in OpenFOAM, specifically Coarse, Medium, Fine, and Finer, with the total number of elements increasing from 9,000 to 140,400 for IBM simulations, and from 2,300 to 147,200 for ALE simulations. The coefficient of drag (Cd) values were monitored once steady-state convergence was achieved and subsequently averaged, as outlined in Table 2. Our results revealed a consistent trend of increasing drag coefficient with finer meshes for both methods, with ALE's Cd rising from 1.3842 on the Coarse mesh to 1.4027 on the Finer mesh, and IBM's from 1.2815 to 1.44, as illustrated in Figure 9. Notably, computational times also increases with mesh refinement, particularly observed in the fine mesh, which was further utilized in subsequent studies. It was observed that IBM simulations were relatively more time-consuming compared to ALE simulations.

The Coefficient of Lift (Cl) and Coefficient of Drag (Cd) data obtained from the Arbitrary Lagrangian-Eulerian (ALE) simulations demonstrated consistent results, particularly with medium, fine and finer mesh qualities. Also, these meshes exhibited similar phases in von Karman vortex generation, indicating synchronized and stable vortex shedding patterns having same amplitude, as shown in Figure 10. Conversely, the coarse mesh in IBM simulations revealed significantly inaccurate Cd and Cl values, suggesting a dependency on finer meshes for precise calculations. However, for IBM, a phase difference in Cl values was observed over time, indicating variations in the timing

of vortex shedding across different mesh sizes, as shown in Figure 11. This highlights the critical influence of mesh quality on the accuracy of aerodynamic coefficients in IBM simulations, underscoring the need for careful mesh selection to capture complex flow dynamics accurately.

Table 2: Grid size convergence test for ALE and IBM Methods

Parameter						
Mesh	**Coefficient of Drag (Cd)**		**Computational Time (s)**		**Number of Elements**	
	ALE	IBM	ALE	IBM	ALE	IBM
Coarse	1.384218	1.2815	144	2674	2300	9000
Medium	1.398152	1.425	592	11528	9200	36000
Fine	1.402569	1.44	3397	35735	36800	81000
Finer	1.402687	1.44	25499	88540	147200	140400

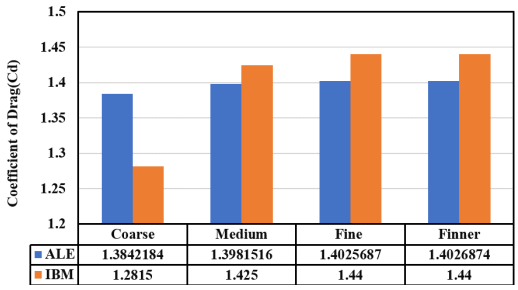

Figure 9: Grid size convergence test for ALE and IBM Methods

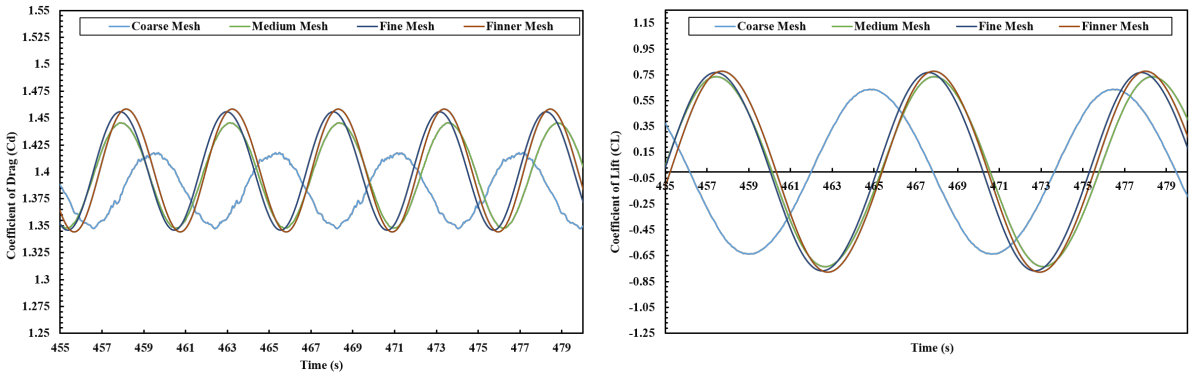

Figure 10: Grid size convergence test- a) Coefficient of Drag (Cd)-Left, and b) Coefficient of Lift (Cl)-Right for ALE at Re=200

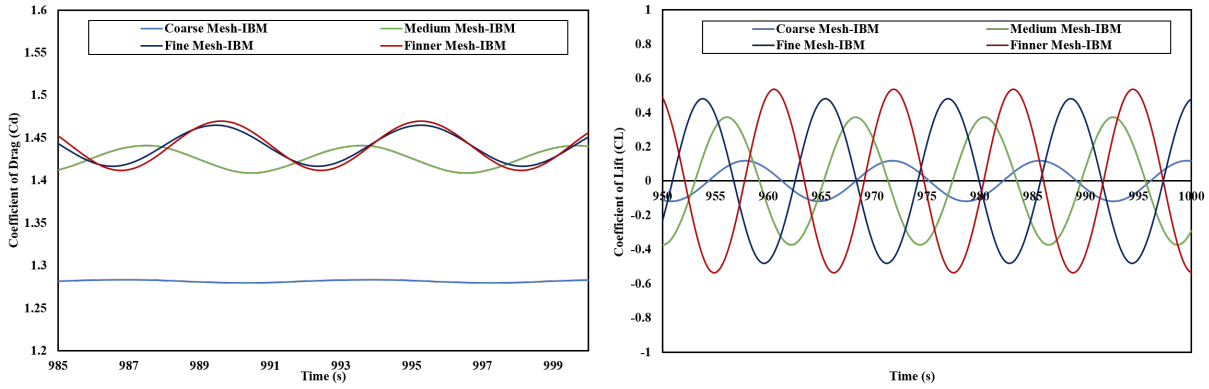

Figure 11: Grid size convergence test- a) Coefficient of Drag (Cd)-Left, and b) Coefficient of Lift (Cl)-Right for IBM at Re=200

3.2 Validation

we assessed the accuracy of our computational fluid dynamics models by comparing the coefficient of drag (Cd) values obtained at Reynolds number 200 with values reported in existing literature [1] [2] [3] [4] [5], as outlined in Table 3. This comparison is essential for verifying the models capability to predict flow behavior accurately under specified conditions. Our CFD study utilized the Arbitrary Lagrangian-Eulerian (ALE) and Immersed Boundary Method (IBM) models, which yielded Cd values of 1.402 and 1.44, respectively. The Cd values from the present study generally fall within the range of values reported in the literature [1] [2] [3] [4] [5], particularly when considering the associated uncertainties. The developed CFD models were further considered for studying the influence of varying Reynolds number on cylinder's aerodynamic performance.

Table 3: Comparison of c_d Values at Re = 200 with literature.

ALE (Present Study)	1.402 – **Re = 200**
IBM (Present Study)	1.44 – **Re = 200**
Reference	c_d **– Re = 200**
[5] Russel and Wang	1.29 ± 0.022
[2] Calhoun and Wang	1.17 ± 0.058
[1] Braza et al.	1.40 ± 0.05
[3] Choi et al.	1.36 ± 0.048
[4] Liu et al.	1.31 ± 0.049

3.3 Results

The influence of varying Reynolds numbers on the aerodynamic performance of a static cylinder was assessed using IBM and ALE approach. The simulations employed IcoFoam (laminar model), PimpleFoam (laminar model), and PimpleFoam with the k-omega SST model. The study was conducted across four Reynolds numbers: laminar flow at Re 100 and 200, and transitional/turbulent flow at Re 1000 and 2000.

For Reynolds numbers 100 and 200, which are within the laminar flow regime, the models predicted C_d values closely aligned with those published in the literature [1] [2] [3] [4] [5]. However, for higher Reynolds numbers (1000 and 2000), which represent transitional flow, slightly higher predictions were obtained using the ALE with the laminar model. This necessitated the deployment of the k-omega SST turbulence model with PimpleFoam to capture more accurately the transitional turbulence flow around the cylinder.

The results from IBM with the laminar model and ALE with the k-omega SST model produced closely aligned C_d values. Specifically, C_d values of 1.5 and 1.44 were predicted using IBM, whereas a C_d value of 1.4 was observed with the ALE-IcoFoam solver. The PimpleFoam laminar model estimated C_d values at 1.38 and 1.375. In cases of Re 1000 and 2000, C_d values were 1.287 and 1.143 using IBM, and for PimpleFoam with the k-omega SST model, the values were 1.374 and 1.29, respectively as outlined in Table 4. These results indicate that C_d values decrease with an increase in Reynolds number for flow around a static cylinder, consistent with findings reported in the literature [24], also illustrated in Figure 12.

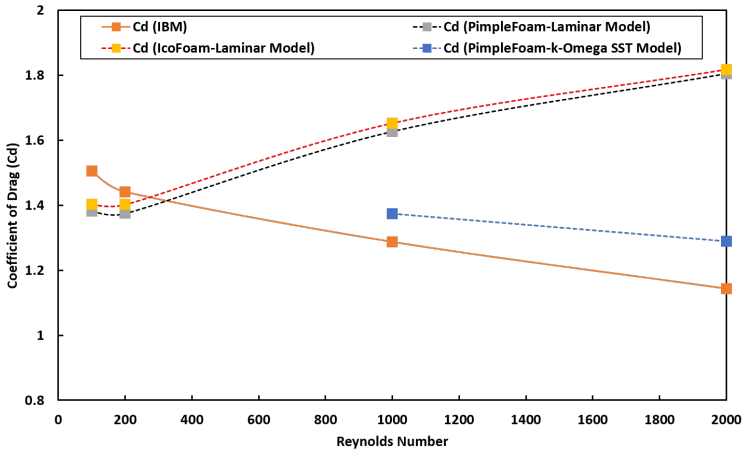

Figure 12: Influence of varying Reynolds number on the aerodynamic performance of cylinder comparision between ALE and IBM

Table 4: Coefficient of Drag (Cd) Across Different Models and Reynolds Numbers.

Re	IBM	IcoFoam Laminar Model	PimpleFoam Laminar Model	PimpleFoam k-Omega SST Model
100	1.505	1.402	1.382	-
200	1.441	1.402	1.375	-
1000	1.287	1.652	1.627	1.374
2000	1.143	1.817	1.805	1.29

The instantaneous Cl and Cd plots indicate that Cd reduces with an increase in Reynolds number, whereas Cl values increase with higher Reynolds numbers. The Cl and Cd plots reveal more dynamic behavior of flow around the cylinder, attributed to the formation of von Karman vortex streets. The findings demonstrate the magnitude of these aerodynamic forces generated over time using different solvers, as illustrated below:

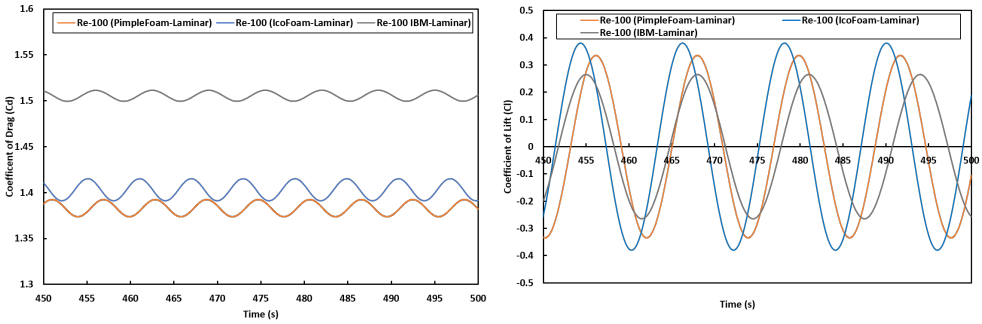

Figure 13: Comparison of a) Coefficient of Drag (Cd)-Left, and b) Coefficient of Lift (Cl)-Right for IBM and ALE at Re=100

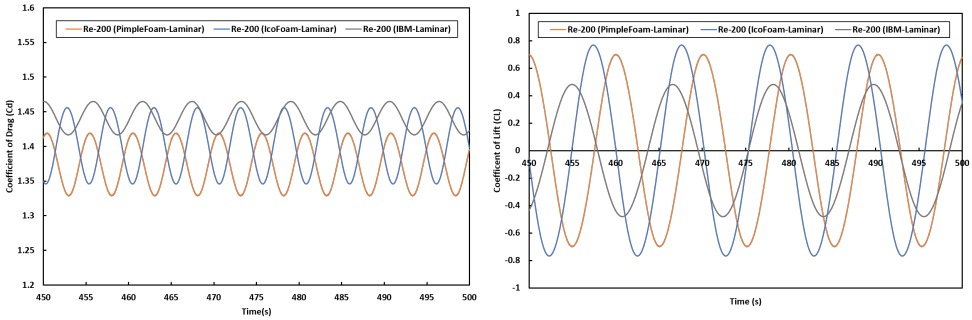

Figure 14: Comparison of a) Coefficient of Drag (Cd)-Left, and b) Coefficient of Lift (Cl)-Right for IBM and ALE at Re=200

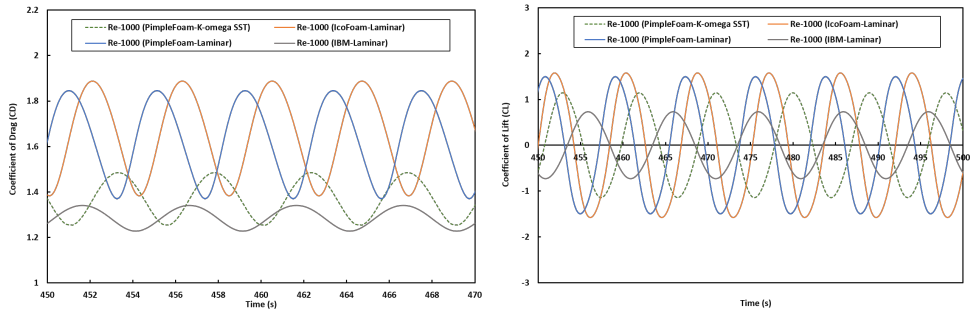

Figure 15: Comparison of a) Coefficient of Drag (Cd)-Left, and b) Coefficient of Lift (Cl)-Right for IBM and ALE at Re=1000

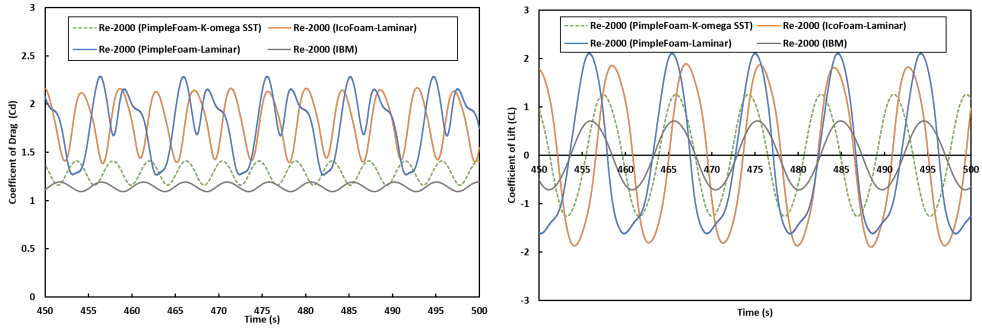

Figure 16: Comparison of a) Coefficient of Drag (Cd)-Left, and b) Coefficient of Lift (Cl)-Right for IBM and ALE at Re=2000

Figure 17 and 18 illustrates the formation of Von Karman vortex generation around a static cylinder at varying Reynolds numbers—Re=100, 200, 1000, and 2000—highlighting the transition from laminar to turbulent flow regimes. At Reynolds numbers Re=100 and Re=200, the flow remains largely laminar, characterized by smooth and steady streamlines with only slight vortex shedding noticeable at Re=200, indicative of the initial stages of flow instability and separation. However, at Re=1000, the flow exhibits a clear shift towards transitional dynamics; the vortex shedding becomes more pronounced and regular, signaling an increased influence of inertial forces over viscous forces, which introduces more complex and periodic oscillations in the wake of the cylinder. By Re=2000, the flow fully enters the early turbulent phase, featuring frequent vortex shedding and chaotic patterns that denote a significant increase in turbulence intensity and wake complexity, also illustrated below:

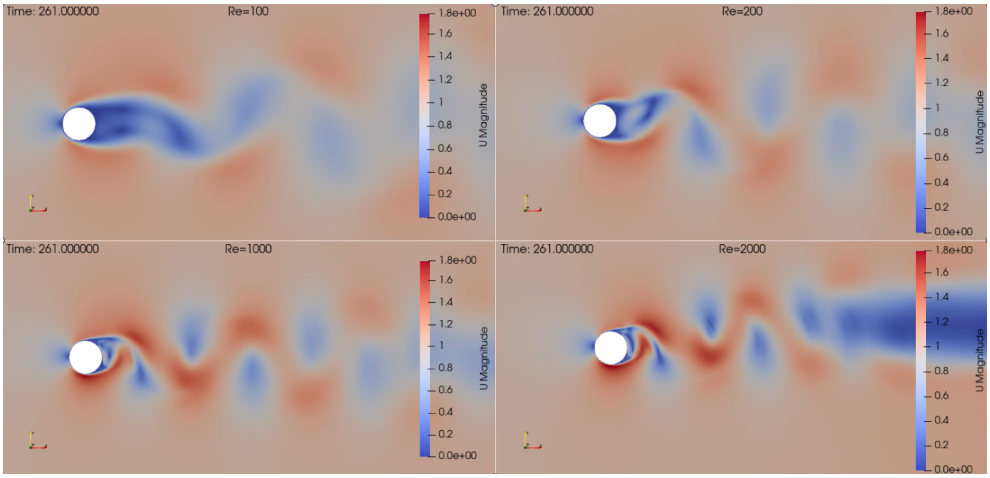

Figure 17: Velocity contours: Illustration of Von Karman Vortex Formation Around a Cylinder at different Reynolds number using ALE

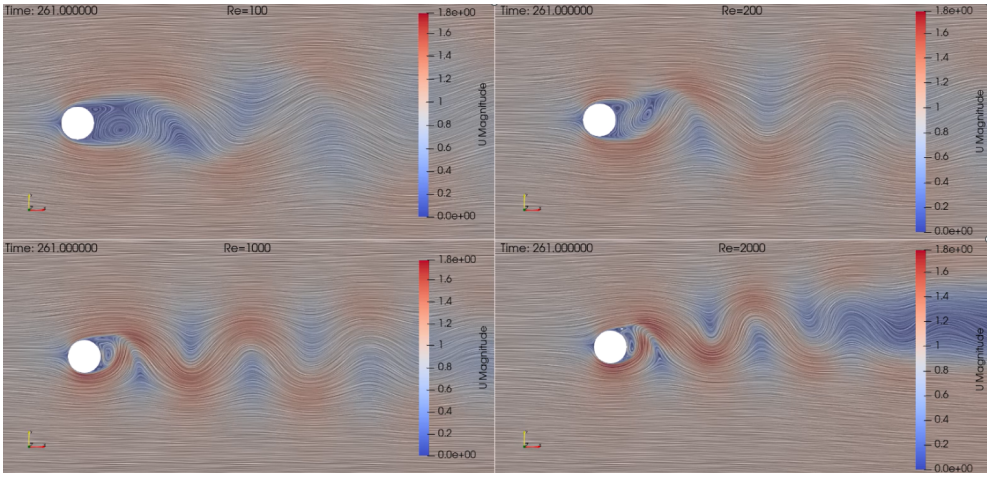

Figure 18: Streamline contours:Illustration of Von Karman Vortex Formation Around a Cylinder at different Reynolds number using ALE

At Re=200, both IBM and ALE methods effectively demonstrate the fundamental phenomenon of vortex shedding behind a cylinder, which is typical for this range of Reynolds numbers. The detailed flow structures captured by both methods are indicative of their respective strengths in resolving the complex dynamics of fluid flow around bluff bodies. IBM shows more confined and structured wake patterns, while ALE provides a broader perspective on flow dispersion, which may be crucial for applications involving extensive fluid-structure interactions, as demonstrated below:

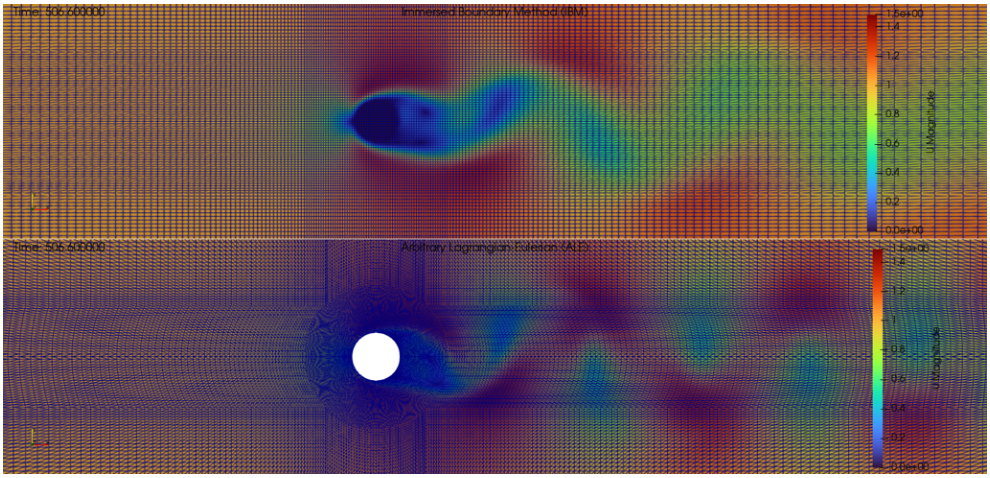

Figure 19: Representation of grid and velocity flow field for ALE and IBM at Re=200

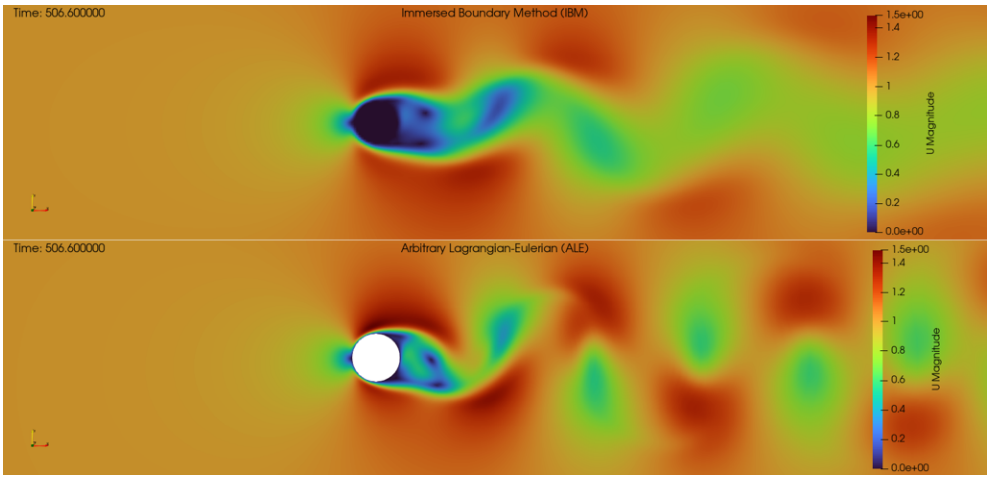

Figure 20: Velocity contours:Illustration of Von Karman Vortex Formation Around a Cylinder at different Reynolds number using ALE and IBM at Re=200

A study on flow around an oscillating cylinder was also conducted for the same cylinder oscillating with a 0.2 m amplitude in the Y-axis at a frequency of 1 Hz. The results indicate that both models are able to capture the flow physics precisely; however, there is a slight variation between the Cl and Cd values. Averaged Cd values of 1.52 and 1.404 were found for ALE and IBM respectively, and this disparity is due to the IBM's inability to accommodate the mesh motion dynamics precisely when it oscillates,as illustrated below:

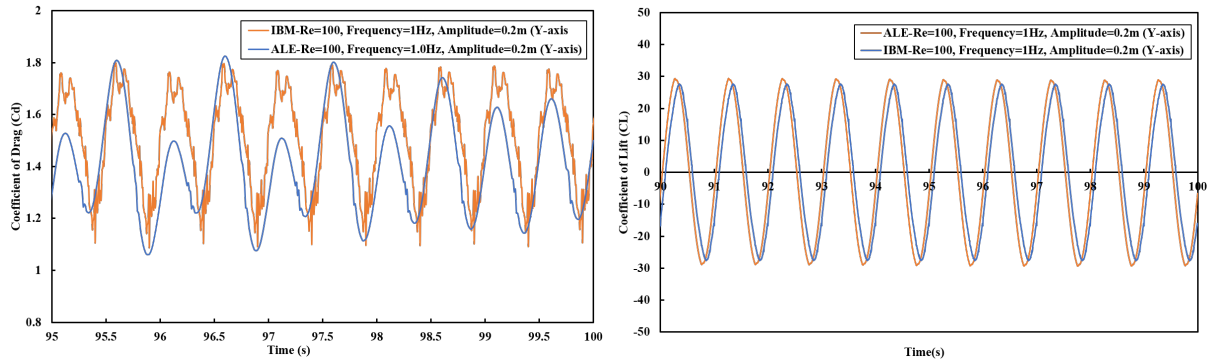

Figure 21: Grid size convergence test- a) Coefficient of Drag (Cd)-Left, and b) Coefficient of Lift (Cl)-Right for IBM at Re=100

A time-dependent and mesh-dependent study was also conducted for the IBM model with a 0.5 Hz oscillating frequency and 0.2 m amplitude in the Y-axis at Re=100. The findings concluded that refining the mesh leads to more fluctuations in the instantaneous values of Cd. Whereas the time-dependent study revealed that having a timestep size of 0.05s produces periodic, smooth oscillations. However, with timestep sizes of 0.01s and 0.005s, dynamic instabilities were observed in the instantaneous values of Cd. This highlights that both the mesh and timestep play important roles in predicting the accurate values of forces around any object while conducting IBM studies.

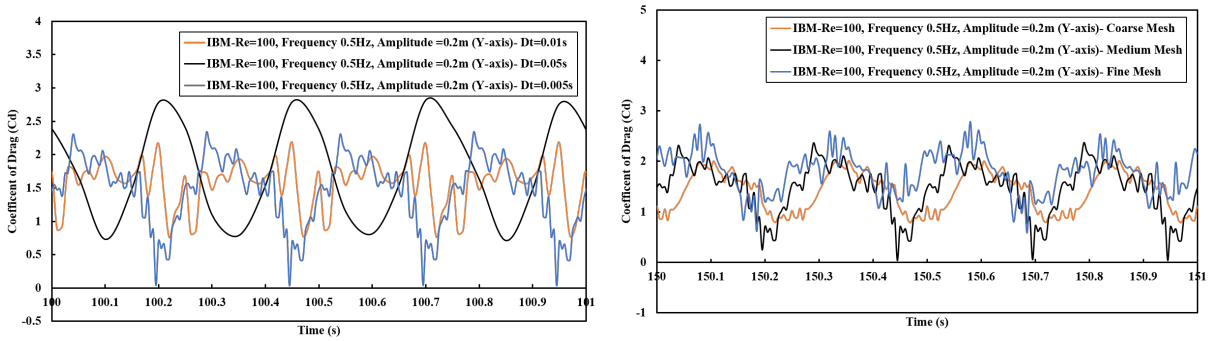

Figure 22: Mesh sensitivity (right) and time step sensitivity(left) test for IBM at Re=100 and 0.5Hz frequency.

4 Conclusions

This study provided a detailed analysis of aerodynamic behaviors around a static cylinder using both the Immersed Boundary Method (IBM) and the Arbitrary Lagrangian-Eulerian (ALE) methods within the OpenFOAM software suite. Through rigorous simulation, each method was evaluated across a range of Reynolds numbers to determine their efficacy in modeling complex fluid dynamics, such as vortex shedding and variations in lift and drag coefficients.

The findings illustrate that both IBM and ALE effectively capture flow phenomena with inherent strengths and limitations. IBM, which allows for complex geometries on simple grids, was found to

be computationally intensive, especially evident at higher Reynolds numbers where the need for accurate turbulence modeling becomes critical. For example, at Re = 2000, IBM struggled with grid independence, requiring finer meshes to approximate turbulent flows accurately, resulting in computational times of up to 88540 seconds for the finest grids. In contrast, ALE's ability to adaptively refine the computational grid near fluid-structure interfaces offered more precise control over mesh deformations but at the cost of increased setup complexity and potential numerical instabilities if not properly managed.

For static cylinder simulations, lower Reynolds numbers (Re = 100 and 200) produced Cd values consistent with theoretical expectations—1.52 for ALE and 1.404 for IBM—highlighting both methods' capability to model laminar flow conditions effectively. However, transitional and turbulent flows at Re = 1000 and 2000 exhibited discrepancies in predicted Cd values (ALE: 1.374, IBM: 1.143 at Re = 2000), underscoring the necessity for employing advanced turbulence models like the k-omega SST to enhance accuracy in higher Reynolds number regimes.

Additionally, oscillatory cylinder studies revealed the importance of mesh and time step optimization in dynamic simulations. For instance, ALE demonstrated better handling of mesh movement dynamics, though it required careful management to prevent instabilities, particularly at a smaller time step of 0.005 seconds, which exposed limitations in temporal resolution.

This study significantly contributes to our understanding of flow dynamics around cylindrical structures and provides practical insights for engineering applications involving similar fluid interactions. Future work should focus on exploring three-dimensional flow impacts and employing hybrid approaches that leverage both IBM and ALE's strengths to overcome current limitations and improve simulation efficiency and accuracy.

5 Acknowledgement

I am deeply grateful to Dr. Chandan Bose for his unwavering support and invaluable mentorship throughout this project. His profound expertise in OpenFOAM and his guidance were pivotal in both shaping the direction and ensuring the successful completion of my work. Dr. Bose consistently made time for extensive discussions, greatly enriching my understanding and bolstering my confidence to tackle complex simulations.

I would also like to extend my heartfelt thanks to Prof. Janani Srree Murallidharan, Mrs. Payal, and Mr. Harish for their insightful feedback and guidance during my internship. Their perspectives were instrumental in refining my approaches and methodologies.

My sincere appreciation goes to my family, whose enduring support and encouragement have been my cornerstone throughout this journey.

Lastly, I am thankful to the entire CFD-OpenFOAM team at FOSSEE (IIT Bombay) for their support throughout this Internship

References

[1] M. Braza, P. Chassaing, and H. H. Minh, "Numerical study and physical analysis of the pressure and velocity fields in the near wake of a circular cylinder," *Journal of fluid mechanics*, vol. 165, pp. 79–130, 1986.

[2] D. Calhoun, "A cartesian grid method for solving the two-dimensional streamfunction-vorticity equations in irregular regions," *Journal of computational physics*, vol. 176, no. 2, pp. 231–275, 2002.

[3] J.-I. Choi, R. C. Oberoi, J. R. Edwards, and J. A. Rosati, "An immersed boundary method for complex incompressible flows," *Journal of Computational Physics*, vol. 224, no. 2, pp. 757–784, 2007.

[4] C. Liu, X. Zheng, and C. Sung, "Preconditioned multigrid methods for unsteady incompressible flows," *Journal of Computational physics*, vol. 139, no. 1, pp. 35–57, 1998.

[5] D. Russell and Z. J. Wang, "A cartesian grid method for modeling multiple moving objects in 2d incompressible viscous flow," *Journal of Computational Physics*, vol. 191, no. 1, pp. 177–205, 2003.

[6] F. M. White, C. Ng, and S. Saimek, *Fluid mechanics*. McGraw-Hill, cop., 2011.

[7] J. I. Hochstein and A. L. Gerhart, *Young, Munson and Okiishi's A Brief Introduction to Fluid Mechanics*. John Wiley & Sons, 2021.

[8] B. M. Sumer *et al.*, *Hydrodynamics around cylindrical strucures*. World scientific, 2006, vol. 26.

[9] P. W. Bearman, "Vortex shedding from oscillating bluff bodies," *Annual review of fluid mechanics*, vol. 16, no. 1, pp. 195–222, 1984.

[10] C. H. Williamson, "Vortex dynamics in the cylinder wake," *Annual review of fluid mechanics*, vol. 28, no. 1, pp. 477–539, 1996.

[11] J. Anderson, "Fundamentals of aerodynamics, ed. tm-h," *Education*, 2010.

[12] M. Alziadeh, *Flow-sound interaction mechanism of a single spirally finned cylinder in cross-flow*. University of Ontario Institute of Technology (Canada), 2017.

[13] H. Schlichting and K. Gersten, *Boundary-layer theory*. springer, 2016.

[14] J. D. Anderson and J. Wendt, *Computational fluid dynamics*. Springer, 1995, vol. 206.

[15] R. Mittal and G. Iaccarino, "Immersed boundary methods," *Annu. Rev. Fluid Mech.*, vol. 37, pp. 239–261, 2005.

[16] V. Väisänen *et al.*, "Immersed boundary method for computational fluid dynamics-a review and verification in openfoam," Master's thesis, 2020.

[17] J. E. Döhler, "An analysis of the immersed boundary surface method in foam-extend," 2022.

[18] C. W. Hirt, A. A. Amsden, and J. Cook, "An arbitrary lagrangian-eulerian computing method for all flow speeds," *Journal of computational physics*, vol. 14, no. 3, pp. 227–253, 1974.

[19] J. Donea, S. Giuliani, and J.-P. Halleux, "An arbitrary lagrangian-eulerian finite element method for transient dynamic fluid-structure interactions," *Computer methods in applied mechanics and engineering*, vol. 33, no. 1-3, pp. 689–723, 1982.

[20] T. J. Hughes, W. K. Liu, and T. K. Zimmermann, "Lagrangian-eulerian finite element formulation for incompressible viscous flows," *Computer methods in applied mechanics and engineering*, vol. 29, no. 3, pp. 329–349, 1981.

[21] T. E. Tezduyar, M. Behr, S. Mittal, and J. Liou, "A new strategy for finite element computations involving moving boundaries and interfaces—the deforming-spatial-domain/space-time procedure: Ii. computation of free-surface flows, two-liquid flows, and flows with drifting cylinders," *Computer methods in applied mechanics and engineering*, vol. 94, no. 3, pp. 353–371, 1992.

[22] A. Gupta, H. A. Abderrahmane, and I. Janajreh, "Flow analysis and sensitivity study of vertical-axis wind turbine under variable pitching," *Applied Energy*, vol. 358, p. 122648, 2024.

[23] R. Stringer, J. Zang, and A. Hillis, "Unsteady rans computations of flow around a circular cylinder for a wide range of reynolds numbers," *Ocean Engineering*, vol. 87, pp. 1–9, 2014.

[24] G. Nellis and S. Klein, *Heat transfer*. Cambridge university press, 2008.